EPJ manuscript No.
(will be inserted by the editor)

Ensembles, Turbulence and Fluctuation Theorem

Giovanni Gallavotti[1] [a]

INFN Roma1 & Accademia dei Lincei

Received: date / Revised version: date

Abstract. The Fluctuation Theorem is considered intrinsically linked to reversibility and therefore its phenomenological consequence, the Fluctuation Relation, is sometimes considered not applicable. Nevertheless here is considered the paradigmatic example of irreversible evolution, the 2D Navier-Stokes incompressible flow, to show how universal properties of fluctuations in systems evolving irreversibily could be predicted in a general context. Together with a formulation of the theoretical framework several open questions are formulated and a few more simulations are provided to illustrate the results and to stimulate further checks.

PACS. XX.XX.XX No PACS code given

1 Introduction.

Many macroscopic systems are modeled by equations of motion which are not reversible due to action of viscous forces, like Navier Stokes fluid equations. And often the equations can be derived from reversible microscopic models (*e.g.* see [18]). The question that is addressed in this work is whether stationary states of such systems could also be described by reversible equations.

In the '80s transport properties of interacting particles systems have been studied by introducing "*thermostat forces*", [19,6,16]: the idea behind the introduction of "non-Newtonian" forces was that the important stationary properties of the system depend on stationarity and not on the way it is achieved. A feature of resulting equations is that often they are reversible, *i.e.* on phase-space a map $x \to Ix$, independent of the forces (typically I is the change of the velocities sign), exists with the property that $I^2x = x$ anticommutes with the time evolution $x \to x(t) = S_t x$ (*i.e.* $IS_t x = S_{-t}x$).

In the case of equilibrium ergodicity is the basis of the theory of equilibrium statistical properties and of their independence of initial conditions; likewise in systems in stationary states (equilibrium or not) chaoticity of their evolutions takes the role of ergodicity and is the key to understand the typical initial state independence of the stationary states properties (with the possibility of a few stationary states, just as in equilibrium at phase transitions at most a handful of different states arise depending on the initial conditions), [22,23].

This did shew that strongly chaotic evolutions may be described equivalently by different equations: a striking example is in [25] in the case of the NS equations and gave rise to several studies in which strong chaoticity was present, [8,9,10].

Here a different view will be presented, pursuing the ideas of the latter references: it is exposed in recent publications and summarized it in Sec.3-5. The purpose is to investigate whether the proposed analysis (so far tested only in few cases) can lead to predict properties of fluctuations that, formally, can be established in reversible systems.

The viewpoint has been that, in the case of systems that are derived from microscopically reversible mechanical equations (like the NS equations), the time reversal symmetry being fundamental cannot be broken and it has to be possible that the same system can be equivalently described by reversible equations (without, of course, going back to the atomic scale description of the motion).

If so it is natural to ask if certain properties of reversible chaotic evolutions can be manifest in irreversible ones, chaotic or not, as the chaos of the microscopic motions at the base of the macroscopic ones will be always active (even when the macroscopic motion is not chaotic, *e.g.* in NS at very low Reynolds number).

The general "equivalence conjecture" is presented in Sec. 3-5 is applied, assuming the validity of the "Chaotic Hypothesis" (CH), [15,12], to predict fluctuations of the dissipation (defined as phase space volume contraction rate) in a simple incompressible NS equation in 2D with periodic b.c. and constant viscosity.

The (new) result is presented in Sec. 7, where a positive test is analyzed. In Sec.8 it is argued that the test should be regarded only as a first step because simulations deal with cases in which the motion seems to involve an attractor that fills the available phase space. The really interesting case occurs at high Reynolds number, *i.e.* at

Send offprint requests to: giovanni.gallavotti@roma1.infn.it

[a] *Present address:* Fisica, Università Roma "La Sapienza" and INFN

small viscosity, where the attractor is really a tiny surface in phase space: from the results of Sec. 7 it appears that much more stringent test are suggested for future work and are possible with the available computer resources.

The equivalence conjecture is intriguing also because, not only it suggests a close analogy between the theory of equilibrium ensembles and the theory of the NS equation stationary states, but it applies as well to 3D while it does not conflict with the possible existence of singularities in 3D-NS: it deals with properties of the NS evolution *regularized* by a UV cut off which become *independent* on the regularization scale if large enough.

A few new tests of the equivalence are also included as supplementary material, with attention to properties of the Lyapunov spectrum not covered by the equivalence conjecture to which it nevertheless appears, surprisingly, closely related. Of particular interest will be the study of the 3D case: some work on it is being done and a few papers (quoted below) are appearing.

2 Navier-Stokes flow in 2D. Notations.

Here we consider the simple case of an incompressible fluid in a periodic container in dimension 2 (2D), review [13,8]. Velocity $\mathbf{u}(\mathbf{x})$ can be expressed via a Fourier's series; if the container side is 2π then:

$$\mathbf{u}(\mathbf{x}) = \sum_{\mathbf{0}\neq\mathbf{k}=(k_1,k_2)\in Z^2} u_{\mathbf{k}} e(\mathbf{k}) e^{-i\mathbf{k}\cdot\mathbf{x}}, \qquad e(\mathbf{k})\cdot\mathbf{k} = 0 \tag{2.1}$$

with $u_{\mathbf{k}} = \overline{u}_{-\mathbf{k}}$ scalars, $\mathbf{k}^\perp = (k_2, -k_1)$, $e(\mathbf{k}) = \frac{i\mathbf{k}^\perp}{|\mathbf{k}|}$

The NS equation for the components $u_{\mathbf{k}}$ is then:

$$\dot{u}_{\mathbf{k}} = \mathcal{E}(u)_{\mathbf{k}} - \nu\mathbf{k}^2 u_{\mathbf{k}} + f_{\mathbf{k}},$$
$$\mathcal{E}(u)_{\mathbf{k}} = -\sum_{\mathbf{k}_1+\mathbf{k}_2=\mathbf{k}} \frac{(\mathbf{k}_2^2 - \mathbf{k}_1^2)\,(\mathbf{k}_1^\perp\cdot\mathbf{k}_2)}{2|\mathbf{k}_1||\mathbf{k}_2||\mathbf{k}|} u_{\mathbf{k}_1} u_{\mathbf{k}_2}, \tag{2.2}$$

Forcing will be supposed to "act on large scale": $f_{\mathbf{k}} \equiv \mathbf{0}$ for $|\mathbf{k}| > K$ for some K. It is convenient to imagine that f is fixed *once and for all* and $\sum_{\mathbf{k}} |f_{\mathbf{k}}|^2 = 1$: below the case $f_{\mathbf{k}} = \overline{f}_{-\mathbf{k}} \neq 0$ only for $\mathbf{k} = \pm\mathbf{k}_0, \mathbf{k}_0 = (2,-1)$ and random phase will be considered.

Hence the *only dimensionless parameter* in the NS equation to which, for brevity, we refer as the "Reynolds number", is $R \equiv \nu^{-1}$. The NS equations will be considered with ultraviolet regularization N, *i.e.* Eq.(2.2) in which all $\neq \mathbf{0}$ waves $\mathbf{k}, \mathbf{k}_1, \mathbf{k}_2$ have components of modulus $\le N$. Of course we are interested in properties which *do not depend on* N at least for large N.

Notable cancellations are expressed by the identities:

$$\sum_{\mathbf{k}} \overline{u}_{\mathbf{k}} \mathcal{E}(u)_{\mathbf{k}} = 0, \quad \sum_{\mathbf{k}} \mathbf{k}^2 \overline{u}_{\mathbf{k}} \mathcal{E}(u)_{\mathbf{k}} = 0 \tag{2.3}$$

which, in the 2D incompressible Euler flow with no stirring (*i.e.* $\nu = 0, f = 0$), imply conservation of energy E and enstrophy $\mathcal{D}$ (*i.e.* $E = \sum_{\mathbf{k}} |\mathbf{u}_k|^2, \mathcal{D} = \sum_{\mathbf{k}} |\mathbf{k}|^2 |\mathbf{u}_{\mathbf{k}}|^2$). The identities Eq.(2.3) remain valid even in presence of the UV cut-off, *i.e.* if all $\neq \mathbf{0}$ components of $\mathbf{k}, \mathbf{k}_1, \mathbf{k}_2$ in Eq.(2.2),(2.3) are restricted to be $\le N$.

3 Ensembles and nonequilibrium fluids

In Statistical Mechanics (SM) equilibrium states of a system can be *equivalently* described by a probability distribution in different ensembles (canonical, microcanonical and others). In the review [13] an analogous paradigm (evolved from the earlier work [8,13,12]) has been proposed to hold for stationary states in fluid mechanics (actually in more general stationary nonequilibria).

The idea (already presented in the earlier publications, mostly in the form of a proposal for a project) is that in the NS equation the same mechanism that is well known in SM could (should) operate: namely there are different probability distributions which assign the same averages to a large class of observables, *i.e.* the "*local* ones depending only on the particles that happen to be in a fixed region L of space, as long as the region is small compared to the total container volume V (ideally infinite).

The proposal is to identify, in NS, the "local observables" with the functions of the velocity field which depend only on the components $u_{\mathbf{k}}$ with $|\mathbf{k}| < K$ with K small compared to the UV cut off N that regularizes the equation (necessary in the 3D case). So N plays the role of the total volume L and K the role of the (arbitrarily fixed) finite volume (physically $K \ll L$).

As in SM completely different distributions describe the same system provided their parameters are suitably fixed. For instance, fixing density $\rho = 1$, you can use the microcanonical distrbution with energy $E = eV$ or the isokinetic distribution with kinetic energy $T = \frac{2}{3\beta}V$ and the two distributions assign *exactly* the same averages to the local observables, provided the constant microcanonical value of the energy equals the average value of the energy in the isokinetic distribution; or, in the microcanonical and canonical equivalence, the total microcanonical energy equals the average canonical energy.

In the following we consider two evolution equations for the fluid.

1) Denote $t \to S_t^{irr,N}\mathbf{u} = \mathbf{u}(t)$ a solution to the NS equations with UV cut-off N. *Time reversal* $I\mathbf{u} = -\mathbf{u}$ is not a symmetry, *i.e.* $IS_t^{irr,N} \neq S_{-t}^{irr,N} I$, because of viscosity $\nu > 0$.

2) Consider also Eq.(2.2), with the same UV regularization:

$$\dot{u}_{\mathbf{k}} = \mathcal{E}(u)_{\mathbf{k}} - \alpha(u)\mathbf{k}^2 u_{\mathbf{k}} + f_{\mathbf{k}} \tag{3.1}$$

but with viscosity ν replaced by a multiplier $\alpha(u)$ designed so that the enstrophy $\mathcal{D}(u) = \sum_{\mathbf{k}} |\mathbf{k}|^2 |\mathbf{u}_{\mathbf{k}}|^2$ *is conserved*. denote $t \to S_t^{rev,N}\mathbf{u} = \mathbf{u}(t)$ the evolution for Eq.(3.1).

In 2D the second Eq.(2.3) yields:

$$\alpha(\mathbf{u}) = \frac{\sum_{\mathbf{k}} \mathbf{k}^2 \overline{f}_{\mathbf{k}} \mathbf{u}_{\mathbf{k}}}{\sum_{\mathbf{k}} |\mathbf{k}|^4 |\mathbf{u}_{\mathbf{k}}|^2} \tag{3.2}$$

which also immediately implies that flows $t \to \mathbf{u}(t) = S_t^{rev,N}\mathbf{u}$ of Eq.(3.1) are *reversible i.e.* $IS_t^{rev,N} = S_{-t}^{rev,N} I$.[1]

[1] In 3D the second of Eq.(2.3) does not hold: see appendix B for the 3D version of Eq.(3.2).

At fixed forcing f, for each choice of the control parameters, *i.e.* $R = \nu^{-1}$ for the irreversible $S_t^{irr,N}$ and D the enstrophy constant for the reversible $S_t^{rev,N}$, a unique stationary distribution $\mu_R^{irr,N}$ or $\mu_D^{rev,N}$ is determined, if ν is mall enough; which yields the statistical properties of the stationary state reached from (volume)-almost all initial $\mathbf{u}$ in the phase space M^N. At small R there might be different stationary states that can be reached with positive probability depending on the initial data $\mathbf{u}$. All such distributions will be collected in "ensembles": $\mathcal{E}^{irr}$ or $\mathcal{E}^{rev}$ rspectively.

The goal is to see whether a $1-1$ correspondence between the distibutions, in the irreversible ensemble $\mathcal{E}^{irr}$ and in the reversible one $\mathcal{E}^{rev}$, can be established so that in the limit $N \to \infty$, *i.e.* removing the UV cut off, corresponding distributions assign the same average value to the local observables.

Existence of a correspondence with the latter property will be called *Equivalence Hypothesis*.

4 Equivalence

The well known difficulty with achieving control of the enstrophy is to be expected to correspond to an evolution of $\alpha(S_t^{rev,N}\mathbf{u})$ with extreme fluctuations at least at large Reynolds number $R = \frac{1}{\nu}$.[2]

This in turn might produce a *homogeneization* phenomenon which could imply that α can be replaced, for practical purposes, by a constant: leading to statistical properties similar to those of the irreversible evolution $S_t^{irr,N}$, at least on *local observables*, *i.e.* observables $O(\mathbf{u})$ depending on $\mathbf{u}$ via its Fourier components $u_{\mathbf{k}}$ with $|\mathbf{k}| < K$ with K fixed (arbitrarily) but $\ll$ than the UV cut off N.

Possibility of equivalent descriptions of stationary states of turbulent fluids arose in the key work [25]: where the NS equation has been shown to be describable, in simulations, by the stationary state of a different fluid equation obtained by imposing on the Euler equation the constraint that the energy content of "each shell" in $\mathbf{k}$-space is set to the value predicted by the 5/3-law.

In the latter reference, at difference with Eq.(3.1), the constraint was imposed via as many multipliers as inertial shells: yet it led to reversible equations of motion which, remarkably, were shown to attribute to several large scale observables averages (*i.e.* local observables in the above sense) sharing the statistical properties obtained from the corresponding irreversible NS.

The following equivalent ensembles description is proposed, see [13] for a review, for the stationary states of the incompressible fluid.

Let $\mathcal{E}^{irr,N}$ be the family of stationary distributions that can be reached by evolving, via the usual NS Eq.(2.2), initial velocity fields $\mathbf{u}$ selected with probability 1 with respect to *(any)* distribution with density $\rho(\mathbf{u})d\mathbf{u}$ on the phase space M^N defined[3] by the Fourier's coefficients $\mathbf{u_k}$ of $\mathbf{u}$. The conceptual importance and the role of the selection criterion, adopted here, has been stressed and used by Ruelle, see the reviews [22,23] and [13].

Existence of the stationary states will be, here, a consequence of a general assumption, *Chaotic Hypothesis*, on systems which are "chaotic" (*i.e.* have some positive Lyapunov exponents), supposed to hold throughout.[4]

At small viscosity $\nu = \frac{1}{R}$, *i.e.* large Reynolds number R, it is expected that there is a unique stationary state (*i.e.* a probability distribution for the local observables) $\mu_R^{irr,N}(d\mathbf{u}) \in \mathcal{E}^{irr,N}$: discussing the (well known, *e.g.* [7]) possible non uniqueness will also be considered later below.

Likewise let $\mathcal{E}^{rev,N}$ be the family of stationary distributions that can be built in the same way via Eq.(3.1): the distributions can be parameterized by the value of the enstrophy $\mathcal{D}$, which is a constant $D = \mathcal{D}(\mathbf{u})$, fixed by the initial datum enstrophy. And for large D it is expected that there will be a unique stationary state $\widetilde{\mu}_D^{rev,N}(d\mathbf{u}) \in \mathcal{E}$.

In [12] it is proposed, "*Equivalence Hypothesis*" (EH for brevity), that in a turbulent regime (*i.e.* at small ν or large D) the above $\mu_\nu^{irr,N}$ for the irreversible flow and $\widetilde{\mu}_D^{rev,N}$ for the reversible will be *equivalent as* $N \to \infty$ *if*

$$\mu_\nu^{irr,N}(\mathcal{D}) = D_N \tag{4.1}$$

i.e. if the enstrophy D_N *in* $\widetilde{\mu}_{D_N}^{rev,N}$ *is the irreversible evolution average of the enstrophy* $\mathcal{D}(S_t^{irr,N}\mathbf{u})$. The D_N in the r.h.s will in general depend on N: remark, however, the *a priori* bound $D < R^2$ for all N valid in 2D (due to Eq.(2.3)).

The precise meaning is that, fixed ν, for *any local observable* $O(\mathbf{u})$ (*i.e.* of large scale, as defined in paragraph after Eq.(3.2)) it will be, under condition Eq.(4.1):

$$\lim_{N\to\infty} \mu_\nu^{irr,N}(O) = \lim_{N\to\infty} \widetilde{\mu}_{D_N}^{rev,N}(O) \tag{4.2}$$

This will be briefly denoted $\mu_\nu^{irr,N} \sim \widetilde{\mu}_D^{rev,N}$.

[2] In 2D (*only*) enstrophy can be controlled but it can grow up to $\nu^{-2} = R^2$, [9, Eq3.2.24].

[3] If the UV cut-off is intended as contraining all components of $\mathbf{k} \neq \mathbf{0}$ to be $|k_i| \le N$, then the real dimension of the space M^N is $4N(N+1)$ if $d = 2$, as for each $\mathbf{k} \neq \mathbf{0}$ there is one complex coordinate, and $\mathbf{u_k} = \overline{\mathbf{u_{-k}}}$.

[4] The formulation goes back to [15], for a review see [10,13]: **Chaotic Hypothesis (CH):***Evolution of a chaotic system is attracted by a smooth surface in phase space and, on it, it is a smooth Anosov system.* "Anosov systems" are too often still misunderstood (or criticized as constructs by "some mathematicians", [16, p.219]) even though the works [27,5] have been popularized in many later publications by the same authors. Still they are the simplest general examples of chaotic motions and should be regarded to play, in chaotic dynamics, the role played in non-chaotic dynamics by the harmonic oscillators. CH implies, [24], existence of a unique stationary state associated with each attractor: it is a "genericity" hypothesis and here it is supposed to hold for the evolutions considered. It is an interpretation of the (weaker) hypothesis that motion near the attractors is a Axiom A system, [22,23].

The analogy with the *equivalence in SM* between canonical and microcanonical ensembles is stressed in [12]: with $\nu, D, N \to \infty$ playing the role of $\beta, E, V \to \infty$ (inverse temperature, energy and 'thermofynamic' limit).

5 Work per unit time

It is worth spending a few words on the energy balance in stationary states: it provides important insights on the equivalence hypothesis (EH).

The work of the stirring force per unit time $W = \sum_{\mathbf{k}} f_{\mathbf{k}} \overline{u}_{\mathbf{k}}$ is a local observable, by the assumption that $f_{\mathbf{k}} = 0$ unless $|\mathbf{k}| < K$ for some fixed K (see paragraph following Eq.(2.2)).

Hence the implication of EH, *i.e.* that Eq.(4.1) implies Eq.(4.2), yields:

$$\mu_R^N(W) = \widetilde{\mu}_{D_N}^{rev,N}(W) \tag{5.1}$$

This is obtained by just multiplying by $\overline{\mathbf{u}}_{\mathbf{k}}$ both sides of the equations Eq.(2.2) (irreversible NS equation) and Eq.(3.1) (reversible NS) and summing over $\mathbf{k}$: with the result

$$\frac{d}{dt}\frac{1}{2}\sum_{\mathbf{k}} |\mathbf{u}_{\mathbf{k}}|^2 = -\gamma \mathcal{D}(\mathbf{u}) + W(\mathbf{u}) \tag{5.2}$$

where $\gamma = \nu$ for $NS^{irr,N}$ or $\gamma = \alpha(\mathbf{u})$, for $NS^{rev,N}$ (the inertial terms cancel[5] exactly, Eq.(2.3)). Averaging, under the condition Eq.(4.1), over time gives in the two cases:

$$\begin{aligned} &\mu_\nu^{irr,N}(W) - \nu \mu_\nu^{irr,N}(\mathcal{D}) = 0, \\ &\mu_{D_N}^{rev,N}(W) - D_N \mu_{D_N}^{rev,N}(\alpha) = 0 \end{aligned} \tag{5.3}$$

Thus the physically appealing Eq.(5.1), consequence of the equivalence hypothesis, provides an important *test* of it via the energy balance in Eq.(5.4). Namely it implies that the multiplier α in Eq.(3.2) has an average $= \nu$:

$$\nu = \lim_{N\to\infty} \mu_{D_N}^{rev,N}(\alpha), \;\; i.e. \;\; \lim_{N\to\infty} R\mu_{D_N}^{rev,N}(\alpha) = 1 \tag{5.4}$$

thus allowing the interpretation of the equivalence in terms of a "homogeneization property", as proposed above. It supports the suggestion that equivalence relies on chaotic evolution of the multiplier α and leads to a first nontrivial test of equivalence: *i.e.* Eq.(5.2) follows from the equivalence condition Eq.(4.1).

This also shows that the equivalence hypothesis could be also formulated replacing Eq.(4.1) with $\nu_N = \mu_D^{rev,N}(\alpha)$ (this time ν will depend on N as D did in Eq.(4.1)) and, in this case, the relation $\lim_{N\to\infty} \mu_{\nu_N}^{irr,N}(\mathcal{D}) = D$ would be a nontrivial test.

The above analysis establishes a $1-1$ correspondence between the elements of the distributions in $\mathcal{E}^{irr}$ and $\mathcal{E}^{rev}$ of stationary states of the two equations in the region of parameters ν, D in which the equations admit a unique stationary distribution (with probability 1 with respect to the choice of initial data with a distribution with density on phase space, called SRB-distributions).

However it is known that often, even with fixed and constant forcing, as it is the case here, the evolution may be attracted by different attracting sets, each with a probability > 0, particularly if ν is large (at fixed N and small Reynolds number), [7].

The hypothesis should then be extended. A natural extension is that the set of extremal (*i.e.* ergodic) stationary states with given ν or D are in $1-1$ correspondence and each pair $\mu_{\nu,\eta}^{irr}, \widetilde{\mu}_{\eta,D}^{rev}$, labeled by an extra index η, is reached as a limit as $N \to \infty$ of $\mu_{\eta,\nu}^{irr,N}, \widetilde{\mu}_{\eta,D}^{rev,N}$ (which might depend on the initial data or even on alternative ways of realizing the UV cut-off). See [12]: a situation analogous to that arising in the theory of phase transitions in Statistical Mechanics, [20], see the related analysis in [26].

6 Equivalence tests

Tests of equivalence can be found in several publications; to mention the most recent: [9,10,11,12,14,13].

As an example a test of the key relation Eq.(5.4) is reported in Fig.1. Fixing the viscosity a $\nu = \frac{1}{R} = 1/2048$ and $N = 31$, *i.e.* 3968 modes:

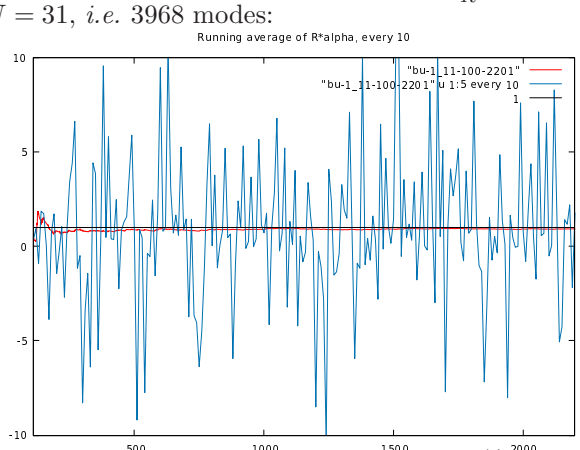

Fig.1: The axis is time in units $2/h$ with $h = 2^{-14}$ as integration time step, with Runge-Kutta-4 integrator. The (blue o.l.) fluctuating line yields the time evolution of the multiplier $R\alpha(t)$ (Eq.(5.4)) in the *reversible evolution* (NS_{rev}); the (red o.l.) line yields at each time t the time average between the initial time up to t, which should be a line asymptotic to 1, which is reached within 10% amid fluctusations 150 times as large in a relatively short (due to computer time constraints) run. And the horizontal line, a visual aid, is the line at height 1. The total run is over $t \in [0, 2200]$ with the time unit which is 2^{15} integration steps each of size 2^{-14}; and the initial data are random while the forcing has only one complex mode, namely $\mathbf{k} = \pm(2, -1)$. Here $R = 2048, N = 31$, 3968 modes (the key numbers are 1=theoretical prediction of the rev.evol. average of $R\alpha(t)$, $11 = \log_2 R$, 100=initial time, 2200=final time).

Fig.1 has been obtained via a semispectral code: in a non spectral method this should be comparable to a 63^2 discretization. Remarkably the same simulation, see [14, fig.2], can be done measuring the multiplier $\alpha(\mathbf{u})$ in the irreversible NS_{irr} evolution, regarding it as an observable

[5] This remains true in 3D NS.

defined by Eq.(3.2): this is not a local observable, still the result is very close to the one in Fig.1. In this case, although α, regarded as an observable for the irreversible NS_{irr} flows, is non local still, in corresponding distributions, its running average has the same average in NS_{rev} and NS_{irr}. This hints at the possible existence of families of non local observables which fall into the equivalence: a point on which to return below.

The same simulation for NS_{rev} can be performed at much larger friction, *e.g.* smaller $R \simeq 28$, and just 48 modes. This time the phenomenology is somewhat different and the variable α undergoes much smaller fluctuations becoming only rarely negative. Equivalence is however respected: increasing viscosity the multiplier α, while strongly fluctuating, will much less fluctuate relatively to its average. Eventually at very large viscosity the flow, in the stationary states, becomes laminar or periodic and fluctuations of α no longer extend to negative values.

Finally it should be stressed that the 2D nature of the equations is *not essential* and all the general ideas carry *unchanged* to 3D: in particular the question of existence and uniqueness of the NS equation in 3D does not arise: the "only" difference is that attention should be really paid to the N dependence of D in Eq.(4.1), no longer constrained by the mentioned *a priori* upper bound. Studies of the 3D reversible NS and its relation with the 3D irreversible are beinning to appear: see [26,1] for NS and [3] for the shell model.

7 Fluctuation Theorem

After the above introduction, summarizing earlier work, consider next the main new question studied in this note. Assuming equivalence it is natural to ask whether reversibility of the NS_{rev} evolution gives new insights in the corresponding NS_{irr} irreversible flows.

Consider the Fluctuation Theorem (FT): for reversible Anosov systems it deals with the phase space contraction (physically interpreted as "entropy production rate", [12]) whose fluctuations exhibit universal properties.

In the NS_{rev} evolution the non constant multiplier α leads to a "phase space contraction" (*i.e.* the "divergence", formally $\sum_{\mathbf{k}} \frac{\partial \dot u_{\mathbf{k}}}{\partial u_{\mathbf{k}}}$) which, after a brief calculation, is:

$$\sigma(u) = \alpha(u)\Big(2K_2 - 2\frac{E_6(u)}{E_4(u)}\Big) + \frac{F(u)}{E_4(u)} \tag{7.1}$$

with α in Eq.(7.1) and $K_2, E_4(u), E_6(u), F(u)$ are:

$$\begin{aligned} 2K_2 &= \sum_{\mathbf{k}} \mathbf{k}^2,\ E_4(u) = \sum_{\mathbf{k}} (\mathbf{k}^2)^2 |u_{\mathbf{k}}|^2, \\ E_6(u) &= \sum_{\mathbf{k}} (\mathbf{k}^2)^3 |u_{\mathbf{k}}|^2,\ F(u) = \frac{\sum_{\mathbf{k}} (\mathbf{k}^2)^2 \overline{f}_{\mathbf{k}} u_{\mathbf{k}}}{E_4(u)} \end{aligned} \tag{7.2}$$

where the sums run over the $\mathbf{k}$ with $|k_i| \le N$, $i = 1, 2$.

In *time reversible Anosov systems* the fluctuations of the divergence satisfy a general symmetry relation. Namely if S_t denotes the evolution and σ_+ the infinite time average of $\sigma(S_t u)$ and

$$p(u) = \frac{1}{\tau} \int_0^\tau \frac{\sigma(S_\theta u)}{\sigma_+} d\theta \tag{7.3}$$

then p has a probability distribution in the stationary state such that $p \in dp$ has density $P(p) = e^{s(p)\tau + O(1)}$, asymptotically as $\tau \to \infty$, with the *universal* symmetry, [15]:

$$s(-p) = s(p) - p\tau\sigma_+ \tag{7.4}$$

called the "Fluctuation Theorem" (FT).

In applications it would be important to know that Eq.(7.4) holds: however in any laboratory experience the relation *cannot* be considered mathematically satisfied because it is essentially impossible to check both the CH *and* the reversibility.

Several attempts can be found to study empirically the relation Eq.(7.4) which, when it cannot be *a priori* proved, is called "Fluctuation Relation" (FR).

Before posing the main question: *is it meaningful to ask whether the FR holds in irreversible evolutions ?* it is necessary studying, first:

1) the probability distribution P of p, defined by Eq.(7.3) both in the reversible and irreversible flows: although p is not a local observable, nevertheless it might be among the non local observables with equal or close corresponding distributions, like the $R\,\alpha$ illustrated in Fig.1, [12,13].

2) the *local Lyapunov spectrum*: defined by considering the Jacobian matrix of the evolution, formally the matrix $J_{\mathbf{k},\mathbf{h}} = \frac{\partial \dot u_{\mathbf{k}}}{\partial u_{\mathbf{h}}}$, and then computing the eigenvalues of its symmetric part, in decreasing order, and averaging each one over the flow, see [21, p.291].

Whether the spectra of the reversible and irreversible evolutions are close is related to the key question: because in reversible Anosov systems the number of exponents ≥ 0 equals that of negative exponents. Hence their equality *indirectly tests CH.*

Preliminarily it should be asked whether the FR is even to be expected at least for the stationary flows obeying reversible NS_{rev}. The CH, which is assumed, will imply that the evolution is a Anosov flow on the attracting surface. However, to apply the theorem, evolution should also be time reversible: and if the attracting set is not the full phase space the FT cannot be applied, at least not without further work.[6]

Hence a simple check will be to count the numbers of positive and negative exponents: if the negative ones are more than the non negative the evolution *on the attracting manifold* cannot be reversible in spite of the time reversibility of NS_{rev} on the full phase space.

The test turns out to be possible, in a reasonable computer time, in the simple case of the NS equation with very few modes, 48 modes and $R = 2048$ (a modest 7×7 grid):

[6] If the attracting surface $\mathcal{A}$, see CH, is not the full phase space M^N then the time reversal image $I\mathcal{A}$ is likely to be disjoint from $\mathcal{A}$ and the motion restricted to $\mathcal{A}$ is not symmetric under the natural time reversal I.

the above defined local Lyapunov spectrum can be equivalently defined as the Lyapunov exponents of the trivial linear flow $S_t v = e^{J^s(\mathbf{u})t}v$: therefore it can be computed either using a packaged routine for the computation of eigenvalues or using (as done here) the algorithm in [2].[7]

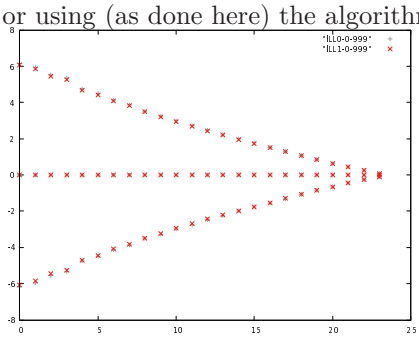

Fig.2: Local Lyapunov spectra for *both* NS_{irr} *and* NS_{rev} flows with $d = 48$ modes, $R = 2048$. Rapid computation with only 1000 samples taken every $4/h$ time steps of time $h = 2^{-13}$ and averaged: the upper and lower values give the $d/2$ exponents λ_k and respectively λ_{d-1-k}, while the middle values are $\frac{1}{2}(\lambda_k + \lambda_{d-1-k})$ not constant but close to $\simeq -.01$. This figure shows positive exponents to be equally numerous as the negative ones and the features **a),b)** listed below.

The quick check in Fig.2 (see also [12,14]) reports $\lambda_k, k = 0 \dots d/2-1$: the first half of the $d = 4N(N+1)$ exponents in decreasing order and the second half $\lambda_{d-1-k}, k = 0 \dots d/2-1$ as function of k (upper and lower curves), as well as $\frac{1}{2}(\lambda_k + \lambda_{d-1-k})$ (intermediate line).

It yields other somewhat surprising results besides showing the equality of the numbers of positive and negative exponents which, as mentioned above, we take as evidence that the attracting set fills densely phase space so that the time reversal symmetry remains a symmetry on the attracting set. Figure draws *in the same panel*, spectra from both NS_{rev} and NS_{irr} flows under equivalence conditions; they apparently ovelap and show:

a) "coincidence" of the spectra of the NS_{rev} and NS_{irr} evolutions: quite surprising and justifying an attempt to formulate and check the Fluctuation Relation in the *irreversible* flows.

b) apparent "pairing": the exponents appear "paired", *i.e.* $\frac{1}{2}(\lambda_k + \lambda_{d-1-k})$ is k-independent. Further results on pairing in the Appendix. Therefore the flow, being reversible and having equal number of pairs of opposite sign, can be consistently assumed to be a Anosov flow and

c) The local Lyapunov spectrum is related to the actual Lyapunov spectrum via interesting inequalities, [21,17]: which could be used to test accuracy of simulations.[8]

The compatibility of the latter result with reversibility suggested to test the FT. The graph for $(s(p)-s(-p))/\sigma_+\tau$ in Eq.(7.4) is studied for both reversible and irreversible flows. It exhibits the main result of this work:

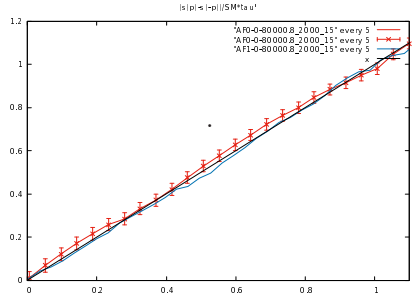

Fig.3: Test the fluctuation relation in the flow NS_{irr} (red o.l.) and NS_{rev} (blue o.l.) flows with 48 modes, $R = 2048$. The τ is chosen 8, the slope of the graph increases with τ reaching 1 at $\tau = 8$. The graph is built with $8 \cdot 10^4$ data, divided into $2 \cdot 10^3$ bins, obtained sampling the flow every $4/h$ time steps of size $h = 2^{-13}$. The keys AF0 and AF1 deal with NS_{irr} (red o.l.) and, respectively, NS_{rev} (blue o.l.) and the error bars (red o.l.) deal with NS_{irr}; the line $f(x) = x$ is a visual aid.

The histogram of the PDF corresponding to Fig.3 is very close to a Gaussian centered at 1 and width yielding the slope of Fig.3:

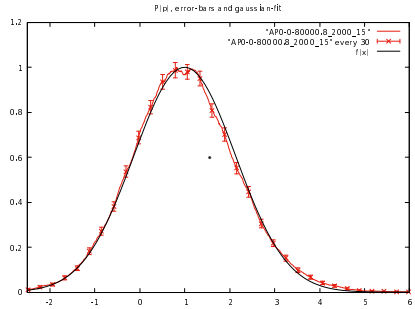

Fig.4: A histogram (with max normalized to 1), of the PDF *for the irreversible flow* of the variable p (red o.l.), with $\tau = 8$ generating the Fig.3 out of the $8 \cdot 10^4$ measurements of $\sigma(\mathbf{u})$ in the NS_{rev}, NS_{irr} equations. The p-axis is divided in 2000 bins and for each p the average of the number (and corresponding error bars) of points in $[p-\delta, p+\delta]$ is plotted (red o.l.) with $\delta = 15/2000$ (corresponding to a small interval of p compared to the width $2\sqrt{\sigma_+\tau}$) and the interpolating Gaussian (blue o.l.). The error bars for the reversible flow (not drawn) have the same sizes.

Fig.3 also shows that the proposed equivalence *extends* also to the phase space contraction ("entropy production rate", [10,12]) as a quantity defined for the reversible evolution but regarded as an observable for the irreversible

[7] Fast in this case, if the time series $\mathbf{u}(t)$ is available (which is provided by the simulations needed to draw graphs like Fig.1) because $\mathbf{u}$, hence, $J(\mathbf{u})$ remain fixed: they are here computed by iterating a large number k of times (of the order of h^{-1}) the matrix $(1 + hJ^s(\mathbf{u}))$ and applying the quoted method. To obtain k-independent results the time series should be taken at time intervals large enough. Within the graph one should recognize one exponent 0 in the NS^{irr} and two in NS^{rev}: but the relative errors are large precisely near $\lambda_k = 0$ and blur this property (to visualize the error sizes in the problem see Fig.8 of the Appendix A, and Fig.6,7,8, which illustrate the almost identity of the average local spectra amid impressive fluctuations particularly in the reversible evolutions).

[8] The inequalities do not estimate the number of positive exponents proportionally to the enstrophy, not even in dimension 2; a question is whether such a bound could hold in dimension 2 by allowing a proportionality constant $(\log N)^c$ for some c.

NS. The interest of the result in Fig.3 is to provide an *a priori* predicted fluctuation relation in a *irreversible* evolution.[9]

8 Problems on strong dissipation

The results on the fluctuation relation (FR) are very special because the UV regularization is so small that the number of (local) Lyapunov exponents can be easily computed and checked to be the same for negative and non-negative ones. This makes possible to suppose that CH holds and that the attracting surface is the entire phase space, so that time reversal is a symmetry for the evolution on the attractor: which implies that the FR follows from the FT and leads to the above test.

More interesting would be the case of higher regularization: already at 224 modes the number of negative exponents *exceeds* that of the positive ones. The first remark is that, nevertheless, the (approximate) "pairing" between exponents already quite clear in Fig.2 remains a characteristic feature, as the cut-off N increases, see Fig.5 below.

Three objections can be raised, before even beginning to attempt possible application of the FT to NS evolutions with strong dissipation and several momentum scales.

1) excess of negative Lyapunov exponents which indicates (if CH holds) that the flow evolves towards an attractor of dimension smaller than the full dimension of phase space: this breaks time reversal symmetry which ceases to be a symmetry of the evolution on the attractors (although it *remains* a global symmetry for the NS_{rev} flows).

2) if the attracting set dimension is lower than that of phase space, the contraction to which the FT *might apply* under the CH is not the full divergence of the equations of motion: one should rather consider the contraction of the surface of the attracting set.

3) the fluctuation theorem does not apply to irreversible evolutions, like NS_{irr}, not even if CH holds.

Results on the determination of the local exponents spectrum in a 960 truncation of the NS_{rev} and NS_{irr} equations at high Reynolds number $R = 2048$ are:

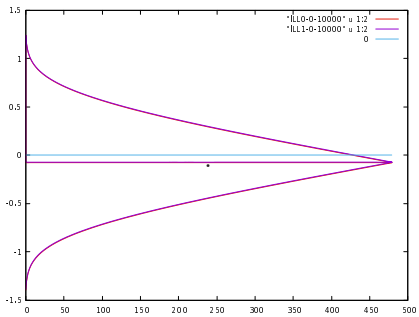

A

Fig.5: The local Lyapunov spectrum in a 960 modes in NS_{rev} and NS_{irr} flows at $R = 2048$. The $n = 4N(N+1)$ exponents $\lambda_0, \dots \lambda_{n-1}$ are drawn reporting for each $k = 0, \dots, k_{\frac{n}{2}-1}$ the values of $\lambda_k, \lambda_{n-1-k}$ and the average $\frac{1}{2}(\lambda_k + \lambda_{n-1-k})$ for each $k = 0, \dots \frac{n}{2} - 1$ ("pairing curve"). The spectra are averaged over a time 800 units sampled every 4 (quite short): before reaching such times the running average values have become stable, although the individual exponents are still fluctuating. Also remarkable is the *apparent* "pairing" between $\lambda_k, \lambda_{n-1-k}$: however this pairing is approximately realized only in a range of R and N: if R is lowered at fixed N the pairing line becomes *sensibly curved* (as checked) and the same should happen at fixed R and large N. Graphs are "by lines": but also "by points" would look continuous because n is large.

Fig.5 gives the spectra (in the same panel and *almost superposed* on the scale of the drawing) and shows their agreement in corresponding evolutions. The straight line at level 0 is a visual aid (it shows immediately that the sum of the exponents is < 0 and that time reversal *I is not a symmetry* on the attracting surface if CH, which implies that motion should be a Anosov flow,x holds).

Fig.5 exhibits a *large number* of observables (*i.e.* the individual Lyapunov exponents) which, although non local as observables, have the "same average" values in corresponding stationary states: namely the 960 local Lyapunov exponents in the 2D case of Fig.5 and the PDF's Fig.3 and Fig.4.

Returning to the FR and to the above objections, the latter results on the Lyapunov spectrum suggest a *new viewpoint*.

In [12,13] is has been proposed that the first two objections do not apply to the cases considered here if the following interpretation of Fig.5 is accepted: the exponents which are part of the negative pairs have to be discarded being interpreted as the exponents controlling the uninsteresting attraction by the attracting surface. Hence one remains with an equal number of positive and negative exponents (*i.e.* only the pairs of opposite sign count to evaluate the phase space contraction on the attractor).

The lack of time reversal symmetry applies to the NS_{rev} whenever the attracting set is smaller than the full phase space (as in the case reported in Fig.5) and, of course, *always* to the NS_{irr}. A different time reversal symmetry mapping the attracting surface into itself, could be recovered if the assumption that the flow satisfies Axiom C is accepted, [4,10].

This has not yet been tested: however the approximate (see caption to Fig.5) pairing would be very helpful because it suggests ∼proportionality between the sum of the $2n^*$ exponents appearing in pairs of opposite sign and the sum of all $d = 4N(N+1) \stackrel{def}{=} 2n$ pairs: the latter is directly accessible from the total divergence and the sum of the opposite pairs is identified with the phase space contraction of the attracting set so that average of the latter will simply be

$$\sigma_{attractor,+} = \frac{num.\ of\ opposite\ sign\ pairs}{num.\ pairs}\sigma_+ \stackrel{def}{=} \frac{n^*}{n}\sigma_+ \tag{8.1}$$

The contraction $\sigma_{attractor}$ on the surface of the attracting set at the configuration u is proposed to be identified with

[9] In summary the prediction is based on CH, on the equality of numbers of negative and non negative exponents and on the extension of the equivalence hypothesis to the entropy production rate.

the sum $\sum_{k=0}^{n^*}(\lambda_k(u)+\lambda_{n-k-1}(u))$ of the local exponents. For a physical interpretation and relevance in terms of *entropy generation* of $\sigma_{attractor}$ see [13, Sec.9].

The above comments on problems 1,2,3 could then be tested, at the same time, by checking validity of FR with slope $\frac{n^*}{n}\tau\sigma_+$ rather than $\tau\sigma_+$: this is a difficult (*i.e.* computationally demanding time), not an impossible simulation task, but it has not been tested yet.

Further properties of the local Lyapunov spectra and a large scale representation of the apparent difference between corresponding reversible and irreversible exponents, is illustrated in the drawings in Fig.6&7&8 in the Appendix and in Fig.1&4, Fig.6&7, Fig.1&2 in, respectively, [12,13,14].

A question that needs to be studied is whether the Equivalence Hypothesis extends to 3D, as I conjecture, or more modestly is restricted to 2D; or whether it demands a R growing with the cut-off, so that the scales of the local observables are always below the Kolmogorov's scale. As formulated here, fixed R and a scale above Kolmogorov's scale, equivalence will be eventually realized if N is large enough (an often criticized proposal): this is a key difference between the conjecture formulated in [8] (for cases with N fixed and $R\to\infty$, based on strong chaos) and the one here (for cases with R fixed and $N\to\infty$, based on microscopic chaos and ensembles equivalence).

A Extra plots

Complementary plots illustrate other aspects obtained in auxiliary simulations.

Remarkably individual local exponents have fluctuations in reversible flows much larger than those of corresponfing irreversible flows. This is clearly exhibited in the following figure

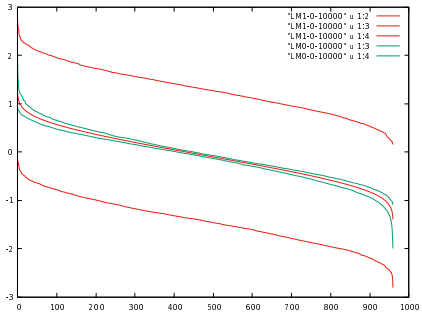

Fig.6: The upper (red o.l.) curve are the loci of the largest values observed, in the time $t\le 10000$ considered in Fig.5, (960 modes, $R=2048$), of the *reversible flow* exponents; lower (red o.l.) curve are loci of smallest values observed and central (red o.l.) line is the actual Lyapunov spectrum for the reversible flow (in Fig.5 curve was drawn breaking it in two halves to exhibit pairing: and in the following fig.7 it is reproduced without breaking it). The two (green o.l.) central lines are the upper and lower values observed in the *irreversible flow* exponents: the drawing shows that the average of the reversible flow is between (actually covered by) upper and lower values of irreversible flow exponents (whose average values are not drawn but on drawing scale would coincide with the reversible flow exponents).

Fig.6 is surprising: the instantaneous local exponents fluctuate very differently: the reversible ones far more than the irreversible ones but they have the same averages. And one could think that, drawing all the instantaneous exponents, in both cases one would fill randomly the space between the upper fluctuation and the lower one. Instead the space would be filled by lines "parallel" to the averages.

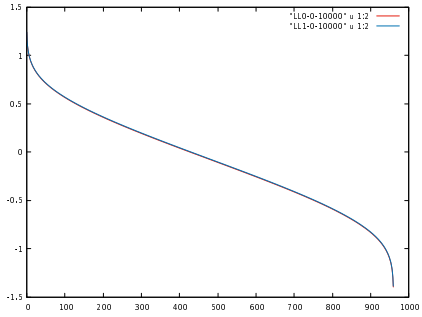

Fig.7: Local Lyapunov spectrum in a 960 modes at $R=2048$ *for both* NS_{rev} *and* NS_{irr} *flows in the same panel*, overlapping (see however Fig.8). The $n=4N(N+1)$ exponents $\lambda_0,\dots\lambda_{n-1}$ for NS_{rev} and NS_{irr} flows are drawn and are apparently *superposed*. Spectra are averaged over a time $4*3600$ units of $4/h$ steps of size $h=2^{-17}$, sampled every 4: before reaching such times the running average values have become stable, although the individual exponents are still fluctuating. See Fig.6 above.

However the two spectra, overlapping in Fig.7, differ as shown in the Fig.8 below.

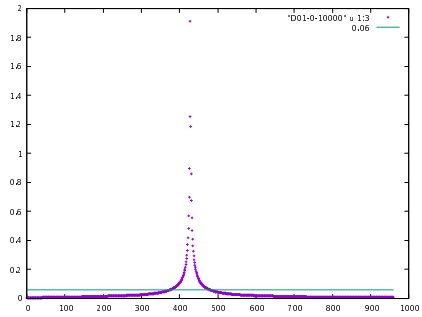

Fig.8: The two spectra in the previous figure are here individually compared term by term, drawing for each $k\in[0,960)$ the difference $\frac{|\lambda_k^{irr}-\lambda_k^{rev}|}{(|\lambda_k^{irr}|+|\lambda^{rev}|)/2}$. The line marks 6%. The larger relative difference at the center of the spectrum mostly reflects that it is there that the exponents are close to zero so that the numerical errors are larger.

Preliminary results on the local Lyapunov spectrum in a 3968 modes truncation are in the graph in Fig.8: this is a difficult computation due to the computer time necessary.

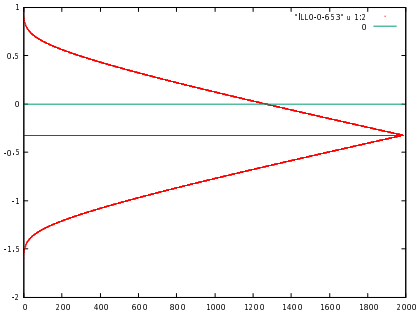

Fig.9: The NS_{irr} local Lyapunov spectrum as in Fig.2 but for a large truncation (3968 modes). Still shows a rather clear (approximate) pairing. The same spectrum for the NS_{rev} case is close although appreciably different on the drawing scale: the problem is that the number of modes is very large and the exponents are averaged over a relatively small time span ($t = 800$ while in Fig.7 it is $t = 10000$) due to the computer time need.

B Irreversible and reversible 3D NS

In dimension $d = 3$ the velocity field is represented as

$$\mathbf{u}(\mathbf{x}) = \sum_{\mathbf{0}\neq\mathbf{k}\in Z^3} \mathbf{u}_{\mathbf{k}} e^{-i\mathbf{k}\cdot\mathbf{x}}, \quad \mathbf{u}_{\mathbf{k}} = \sum_{\theta=\pm1} u_{\theta,\mathbf{k}} e_\theta(\mathbf{k}) \tag{B.2}$$

with $u_{\mathbf{k},\theta} = \overline{u}_{-\mathbf{k},\theta}$ scalars, and $e_\theta(\mathbf{k}) = e_\theta(-\mathbf{k}), \theta = \pm1$ are two mutually orthogonal unit vectors in the plane orthogonal to $\mathbf{k}$: $e_\theta(\mathbf{k}) \cdot e_{\theta'}(\mathbf{k}) = \delta_{\theta,\theta'}$.

The Euler equation for the components $u_{\theta,\mathbf{k}}$ is then

$$\dot{\mathbf{u}}_{\mathbf{k}} = \mathcal{E}(\mathbf{u})_{\mathbf{k}}, \qquad \mathcal{E}(\mathbf{u})_{\theta,\mathbf{k}} = \sum_{\mathbf{k}_1+\mathbf{k}_2=\mathbf{k}} (i\mathbf{k}_2 \cdot e_{\theta_1}(\mathbf{k}_1))(e_{\theta_2}(\mathbf{k}_2) \cdot e_\theta(\mathbf{k})) u_{\theta_1,\mathbf{k}_1} u_{\theta_2,\mathbf{k}_2} \tag{B.3}$$

The helicity conservation follows by checking that $\frac{d}{dt}\int \mathbf{u}(\mathbf{x}) \cdot (\boldsymbol{\partial} \wedge \mathbf{u}(\mathbf{x}))\, d\mathbf{x} = 0$.

The reversible version of the 3-dimensional NS equations, in which enstrophy is a constant of motion, is $\dot{\mathbf{u}}_{\mathbf{k}} = \mathcal{E}_{\mathbf{k}}(\mathbf{u}) - \alpha(\mathbf{u})\mathbf{k}^2\mathbf{u}_{\mathbf{k}} + \mathbf{f}_{\mathbf{k}}$ with α defined by:

$$\alpha(\mathbf{u}) = \frac{\big(\sum \mathbf{k}^2\,(\mathbf{u}_{\mathbf{k}_1}\cdot i\mathbf{k}_2)(\mathbf{u}_{\mathbf{k}_2}\cdot\mathbf{u}_{-\mathbf{k}})\big) + \big(\sum_{\mathbf{k}} \mathbf{k}^2 f_{\mathbf{k}}\cdot\mathbf{u}_{-\mathbf{k}}\big)}{\sum_{\mathbf{k}} \mathbf{k}^4 |\mathbf{u}_{\mathbf{k}}|^2} \tag{B.4}$$

where the firs sum runs over $\mathbf{k}_1, \mathbf{k}_2, \mathbf{k}$ with $\mathbf{k} = \mathbf{k}_1 + \mathbf{k}_2$.

Acknowledgements: I am grateful to L.Biferale (Roma2), L.S.Young (CIMS), and to L.Silvestrini (Roma1-INFN) for support and for making available use of their clusters.

References

1. A. Alexakis and M.E. Brachet. Energy fluxes in quasi-equilibrium flows. *arxiv:1906.0272*, preprint:1–15, 2019.
2. G. Benettin, L. Galgani, A. Giorgilli, and J. Strelcyn. Lyapunov charateristic exponents for smooth dynamical systems and for Hamiltonian systems; A method for computing all of them. Part 2, Numerical application. *Meccanica*, 15:21–30, 1980.
3. L. Biferale, M. Cencini, M. DePietro, G. Gallavotti, and V. Lucarini. Equivalence of non-equilibrium ensembles in turbulence models. *Physical Review E*, 98:012201, 2018.
4. F. Bonetto and G. Gallavotti. Reversibility, coarse graining and the chaoticity principle. *Communications in Mathematical Physics*, 189:263–276, 1997.
5. R. Bowen and D. Ruelle. The ergodic theory of axiom A flows. *Inventiones Mathematicae*, 29:181–205, 1975.
6. D. J. Evans and G. P. Morriss. *Statistical Mechanics of Nonequilibrium Fluids*. Academic Press, New-York, 1990.
7. V. Franceschini, C. Giberti, and M. Nicolini. Common Periodic Behavior in larger and larger yruncations of the Navier-Stokes. *Journal of Statistical Physics*, 50:879–896, 1988.
8. G. Gallavotti. Dynamical ensembles equivalence in fluid mechanics. *Physica D*, 105:163–184, 1997.
9. G. Gallavotti. *Foundations of Fluid Dynamics*. (second printing) Springer Verlag, Berlin, 2005.
10. G. Gallavotti. *Nonequilibrium and irreversibility*. Theoretical and Mathematical Physics. Springer-Verlag, 2014.
11. G. Gallavotti. Finite thermostats in classical and quantum nonequilibrium. *European Physics Journal Special Topics*, 227:217–229, 2018.
12. G. Gallavotti. Navier-stokes equation: irreversibility turbulence and ensembles equivalence. *arXiv:1902.09610*, page 09160, 2019.
13. G. Gallavotti. Nonequilibrium and Fluctuation Relation. *Journal of Statistical Physics*, online-first:1–55, 2019.
14. G. Gallavotti. Reversible viscosity and Navier–Stokes fluids. *Springer Proceedings in Mathematics & Statistics*, 282:569–580, 2019.
15. G. Gallavotti and D. Cohen. Dynamical ensembles in nonequilibrium statistical mechanics. *Physical Review Letters*, 74:2694–2697, 1995.
16. W. Hoover. *Time reversibility Computer simulation, and Chaos*. World Scientific, Singapore, 1999.
17. E. Lieb. On characteristic exponents in turbulence. *Communications in Mathematical Physics*, 92:473–480, 1984.
18. J.C. Maxwell. On the dynamical theory of gases. *In: The Scientific Papers of J.C. Maxwell, Cambridge University Press, Ed. W.D. Niven, Vol.2*, pages 26–78, 1866.
19. S. Nosé. A unified formulation of the constant temperature molecular dynamics methods. *Journal of Chemical Physics*, 81:511–519, 1984.
20. D. Ruelle. *Statistical Mechanics*. Benjamin, New York, 1969, 1974.
21. D. Ruelle. Large volume limit of the distribution of characteristic exponents in turbulence. *Communications in Mathematical Physics*, 87:287–302, 1982.
22. D. Ruelle. *Elements of differentiable dynamics and bifurcation theory*. Academic Press, New-York, 1989.
23. D. Ruelle. *Turbulence, strange attractors and chaos*. World Scientific, New-York, 1995.
24. D. Ruelle. La théorie ergodique des systèmes dynamiques d'Anosov. *Leçons de mathématiques d'aujourd'hui (ed. F. Bayart and E. Charpentier), in series: Le sel et le fer, Cassini, Paris*, 4:195–226, 2010.

25. Z.S. She and E. Jackson. Constrained Euler system for Navier-Stokes turbulence. *Physical Review Letters*, 70:1255–1258, 1993.
26. V. Shukla, B. Dubrulle, S. Nazarenko, G. Krstulovic, and S. Thalabard. Phase transition in time-reversible Navier-Stokes equations. *arxiv*, 1811:11503, 2018.
27. Ya. G. Sinai. Construction of Markov partitions. *Functional Analysis and its Applications*, 2(3):70–80, 1968.

.

email: giovanni.gallavotti@roma1.infn.it
web: https://ipparco.roma1.infn.it

Fig.s 1-9 scaled

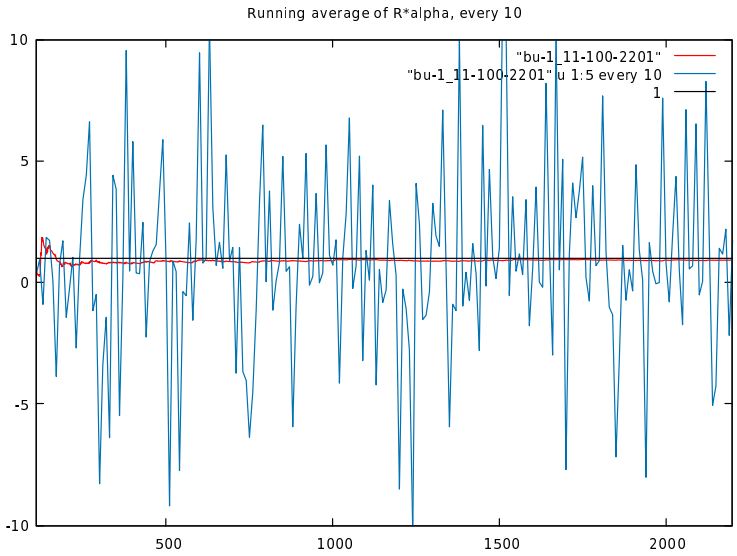

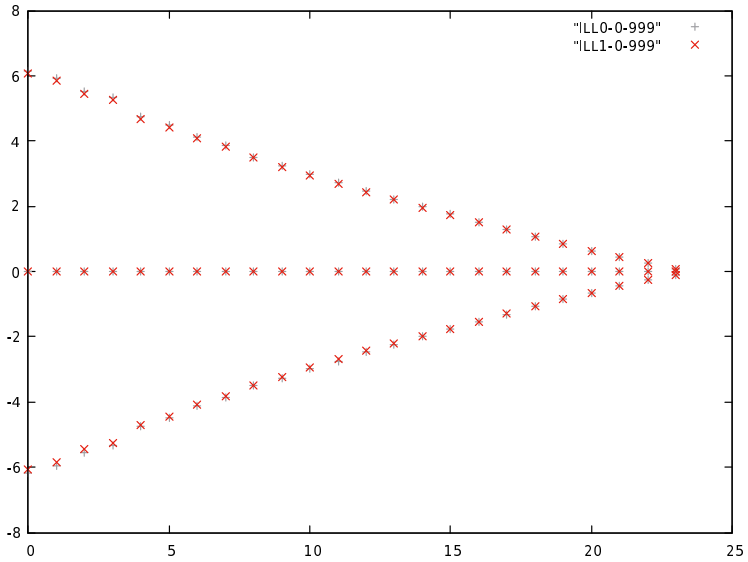

.

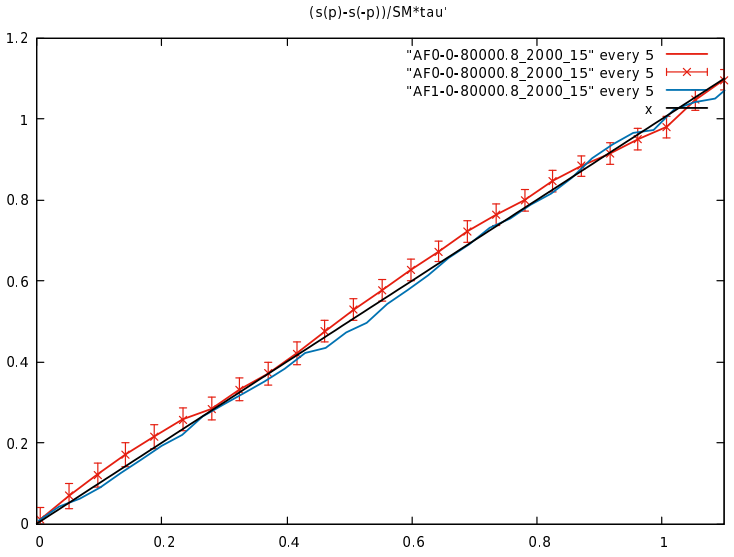
(s(p)-s(-p))/SM*tau'
"AF0-0-80000.8_2000_15" every 5
"AF0-0-80000.8_2000_15" every 5
"AF1-0-80000.8_2000_15" every 5
x
1.2
1
0.8
0.6
0.4
0.2
0
0
0.2
0.4
0.6
0.8
1

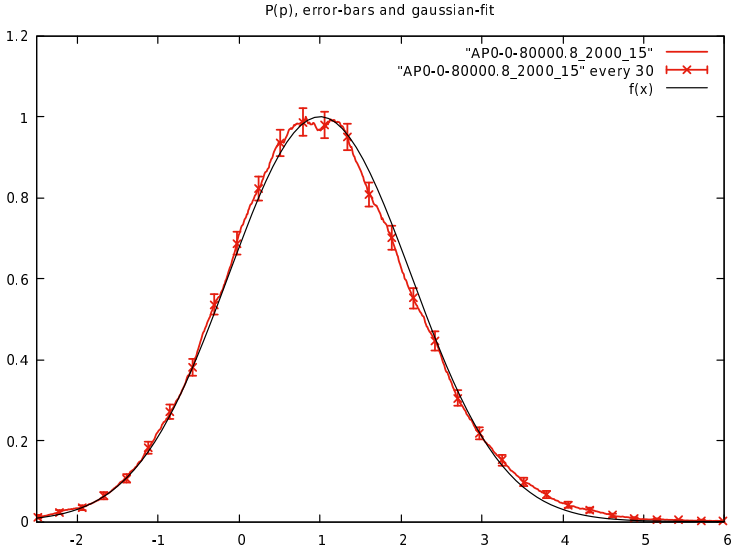
P(p), error-bars and gaussian-fit
"AP0-0-80000.8_2000_15"
"AP0-0-80000.8_2000_15" every 30
f(x)
1.2
1
0.8
0.6
0.4
0.2
0
-2
-1
0
1
2
3
4
5
6

.

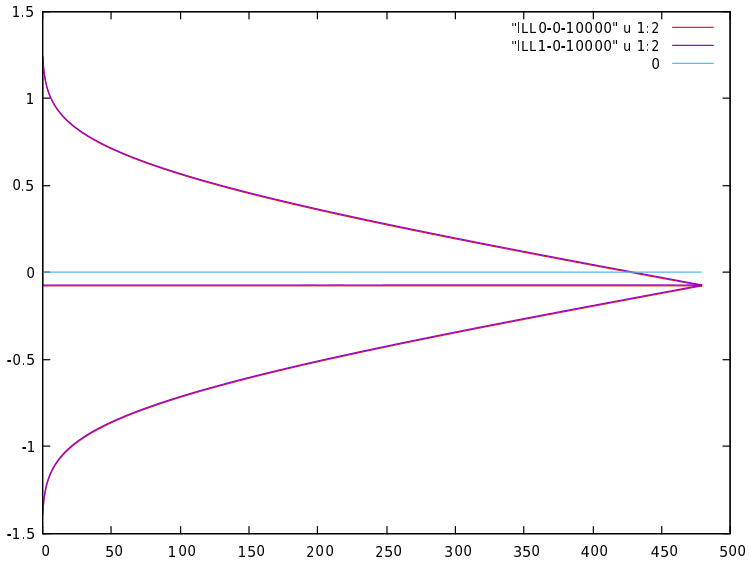
"lLL0-0-10000" u 1:2
"lLL1-0-10000" u 1:2
0
1.5
1
0.5
0
-0.5
-1
-1.5
0
50
100
150
200
250
300
350
400
450
500

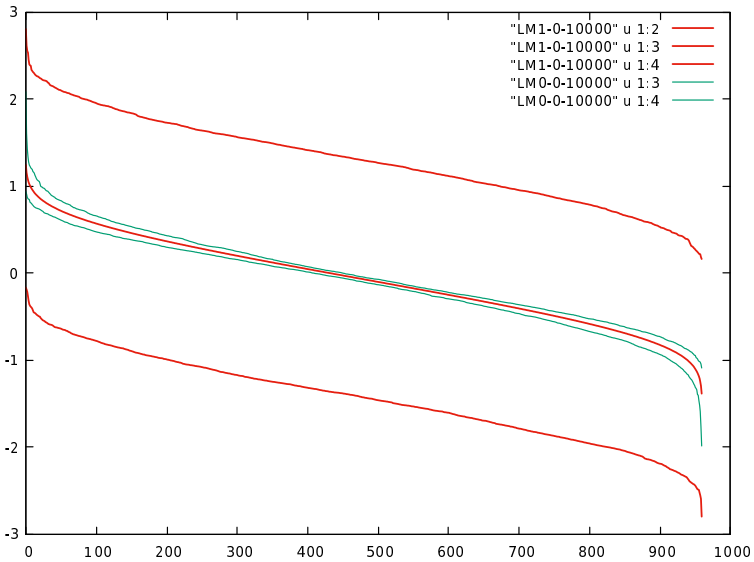
"LM1-0-10000" u 1:2
"LM1-0-10000" u 1:3
"LM1-0-10000" u 1:4
"LM0-0-10000" u 1:3
"LM0-0-10000" u 1:4
3
2
1
0
-1
-2
-3
0
100
200
300
400
500
600
700
800
900
1000

.

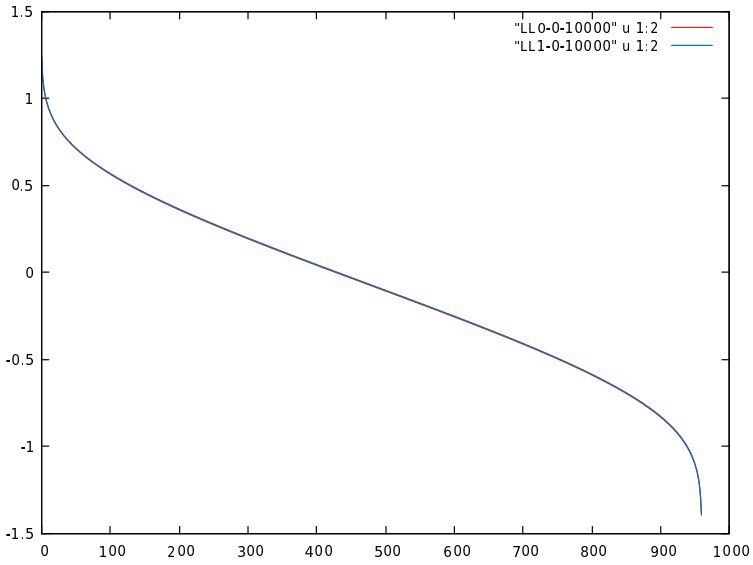
"LL0-0-10000" u 1:2
"LL1-0-10000" u 1:2
1.5
1
0.5
0
-0.5
-1
-1.5
0
100
200
300
400
500
600
700
800
900
1000

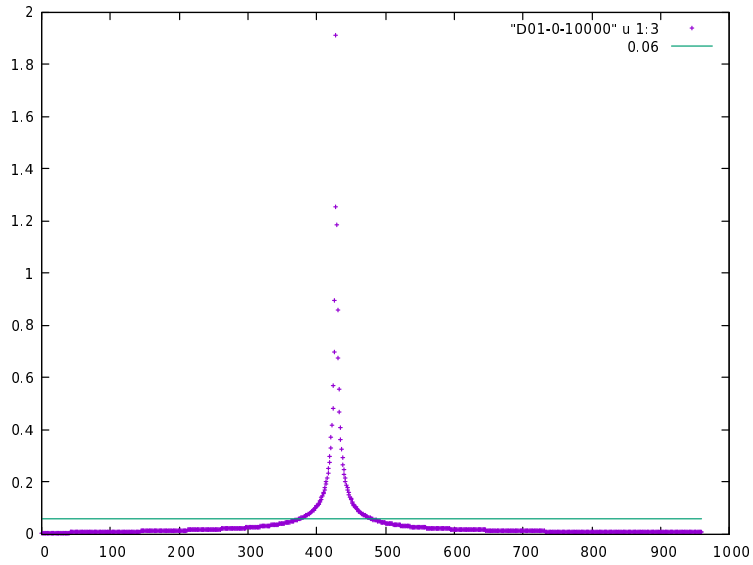
"D01-0-10000" u 1:3
0.06
2
1.8
1.6
1.4
1.2
1
0.8
0.6
0.4
0.2
0
0
100
200
300
400
500
600
700
800
900
1000

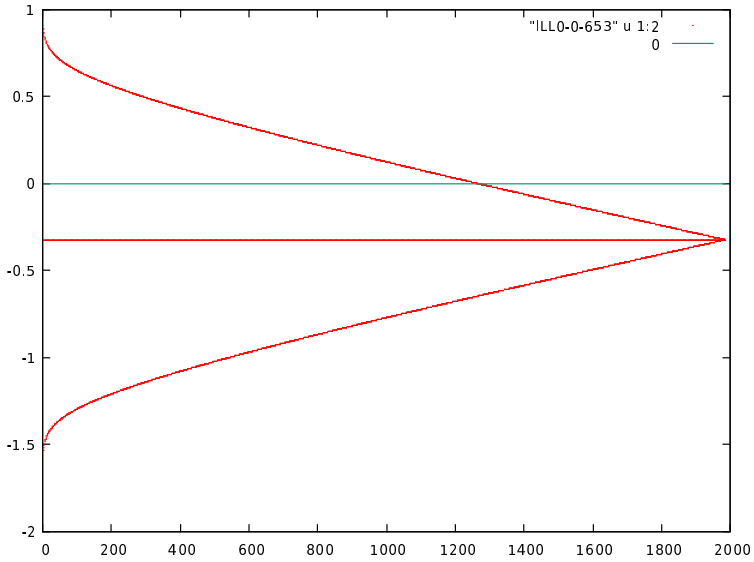
"ILL0-0-653" u 1:2
0
1
0.5
0
-0.5
-1
-1.5
-2
0
200
400
600
800
1000
1200
1400
1600
1800
2000